CIRP Journal of Manufacturing Science and Technology 2 (2010) 170–175

Contents lists available at ScienceDirect

CIRP Journal of Manufacturing Science and Technology

journal homepage: www.elsevier.com/locate/cirpj

Method for online quality monitoring of AWJ cutting by infrared thermography

Andrej Lebar [a], Mihael Junkar [a], Alojz Poredoš [b], Mladen Cvjeticanin [a,*]

[a] Laboratory of Alternative Technologies, Faculty of Mechanical Engineering, University of Ljubljana, Askerceva 6, 1000 Ljubljana, Slovenia
[b] Heat & Mass Transfer and Environmental Studies, Faculty of Mechanical Engineering, University of Ljubljana, Ljubljana, Slovenia

ARTICLE INFO

Article history:
Available online 1 June 2010

Keywords:
Abrasive water jet
Thermography
Monitoring
Adaptive control
Cutting

ABSTRACT

This article presents a novel monitoring method of abrasive water jet (AWJ) cutting process using the infrared thermography. Using this monitoring method it is possible to observe the cutting front in the workpiece and thus to determine the working efficiency of the material removal process. Experimental results showed that it is possible to obtain time versus temperature images which by further computer analysis give better insight in the process and the influence of process setup parameters on the process itself. Complex cybernetic structure was defined in order to achieve adaptive control of AWJ cutting.

1. Introduction

Abrasive water jet (AWJ) is a widely used non-conventional machining process introduced in industrial use less than 30 years ago. It is a mechanical process from the class of energy beam machining technologies such as laser beam machining or plasma cutting. The most important difference from the latter ones is that AWJ is a cold machining process, which yields important consequence that material structure is left unaltered after the machining.

In this paper we report on a method of the AWJ cutting process monitoring using infrared (IR) thermography, a method which online derives AWJ process performance index. In AWJ machining high speed water mixed with abrasive is used to remove the workpiece material. AWJ is used to cut variety of materials with high quality at competitive price. Best results are achieved, when it is applied to thicker materials with complex two-dimensional shapes, regardless of material brittleness, ductility or composition. One of its major attractions is nearly zero heat affected zone.

In contrast with these advantages, workpieces cut with abrasive water jet exhibit a rather random character, which limits its use for accurate machining operations, where tolerances less than 1/20 mm are required. The ability to predict this sort of processes depends largely on the correct definition of contributed mechanisms. Due to the action of high velocity water and hidden material-jet-abrasive interface zone, only few direct measurement methods are possible.

One of few possibilities, which are left to monitor this process, is to observe the workpiece by IR camera and to online process the thermographic image using methods of digital image processing.

Online process monitoring is a first step towards process control, therefore several experimental principles were tested relatively soon after AWJ cutting invention. Hashish performed AWJ cutting process visualization on transparent material polymethyl methacrylate by means of a high speed camera [1]. The experiment clarified to some extent the mechanism of cutting front propagation and proved the existence of a step formation on the cutting front. Hashish [1] suggested that photoelastic study and infrared visualization should be performed. Photoelastic study was performed on transparent birefringent material by Ramulu [2], who identified two distinctive processes: microcracking due to pure water jet and microcrack nucleation and micromachining due to abrasive action. AWJ machining thermal distribution on workpiece was first measured by Ohadi et al. [3], who inserted a matrix of thermocouples in the lateral workpiece surface and bottom surface regarding to the traverse direction of the cutting head movement. It was shown that temperature peaks rose up to 70 °C and found out that caution should be paid when generalizing AWJ as a cold process. The feasibility of monitoring of the AWJ cutting process and the mixing tube wear, by IR thermography was first studied by Kovacevic et al. [4]. Their results are in good agreement with results obtained by Ohadi et al. They performed also the monitoring of the AWJ cutting head, especially mixing tube wear. It was reported that IR thermography is suitable for visualization of cutting mechanisms in opaque materials, but they concluded that the change in traverse speed yields only marginal effect on the temperature distribution in the workpiece.

* Corresponding author. Tel.: +386 14771724; fax: +386 14771759.
E-mail address: mladen.cvjeticanin@fs.uni-lj.si (M. Cvjeticanin).

1755-5817/$ – see front matter © 2010 CIRP.
doi:10.1016/j.cirpj.2010.03.004

We were challenged by these results to find the range of AWJ machining parameters at which different AWJ cutting head speeds would result in significantly different IR thermograms.

2. Thermographic measurements and experimental setup

In our experiment we used IR camera for online monitoring of the AWJ cutting process. Acquired thermograms were afterwards compared to resultant surface texture. Schematic overview of the experimental setup is in Fig. 1.

Experiments were performed on 2-axis AWJ cutting system (type 2652A, OMAX, USA), equipped by high pressure pump (ECOTRON 403, BÖHLER, Austria).

During experiments IR camera (ThermaCam S65, FLIR Systems, USA) was used. ThermaCam S65 has image quality of 320 by 240 pixels and thermal sensitivity 50 mK at 30 °C. Thermal measurement data were sampled with 14 bit precision and were stored in data format suitable for further processing by Matlab software.

The machined material was aluminium alloy 6061-T6, 25.4 mm thick and 46 mm wide (material data in Table 1). Particular material was selected partially to be in correspondence with literature [4] and partially because this material is one of the most frequently machined materials by AWJ. The face of the workpiece, which was turned towards the IR camera, was coated with black enamel of known emissivity. Traverse direction of the cutting head was parallel to the workpiece face exposed to IR monitoring as is shown in Fig. 1. The distance of the cut from the black enamel coated surface of the workpiece was set to 1 mm.

Process parameter varied during experiments was AWJ cutting head traverse rate v_t, which was set to a three different levels (A, B and C level). The selected value for v_t at level A was 3.23 mm/s, at level B 1.74 mm/s and at level C 0.97 mm/s. During the experiment water pressure p, orifice diameter d_o and nozzle diameter d_f were kept constant. Stand-off distance was set to the optimal value [5] for the cutting application h_{so} = 2.5 mm. Abrasive used was garnet type GMA 80 mesh with abrasive mass flow rate set to 5.3 g/s. Process parameters are collected in Table 1. Experiments for the each cutting head traverse rate (A, B, and C) were repeated five times.

The radiation measured by the IR camera depends primary on the temperature of the measured object but is a function of emissivity also. Additionally radiation originates in the surroundings and some part of it is directly or indirectly captured by IR camera. The radiation from the object and the reflected radiation will also be influenced by the absorption of the atmosphere. In order to measure temperature accurately, it is therefore necessary to compensate the measurement for the effects of a number of different radiation sources. The following parameters must be set on the camera in order to measure the temperature of the object precisely: the emissivity of the object ε, the reflected apparent temperature T_{refl} which is the apparent temperature of objects whose radiant energy is reflected off the target into the IR camera, the distance between the object and the camera D, the relative humidity RH and temperature of the atmosphere T_{atm}.

In the preparation phase the workpiece emissivity ε was determined; the reflected apparent temperature T_{refl} was measured according to the IR camera producers protocol; the distance between the object and the camera D was measured using laser distance meter (type PLR 30, BOSCH, Germany). The relative humidity RH and the temperature of the atmosphere T_{atm} were measured with Almemo measuring instrument equipped with hygrometer and temperature sensor (type FHA646-E1C, AHLBORN, Germany). The average relative humidity and temperature of the atmosphere between the IR camera and 1.2 m distant object were $RH = 59.7 \pm 1.2\%$ and $T_{atm} = 20.9 \pm 0.2$ °C, respectively. Reflected apparent temperature $T_{refl} = 20 \pm 2$ °C was determined by using the reflector method proposed by FLIR [6]. Emissivity of the coated workpiece was determined to be $\varepsilon = 0.938 \pm 0.019$. During the experiments, sequences of thermograms were acquired by thermographic camera, recorded and stored for further analysis.

In AWJ cutting process a multiphase jet consisting of abrasive, water and air impacts the surface of cutting front in the workpiece thus eroding the material and simultaneously contributing to the local increase in temperature. Due to thermal conduction of material temperature distribution on the surface of the workpiece resembles to some extent the temperature conditions in the interface zone between workpiece and AWJ.

As it is shown in Fig. 2, the experimental phase of our work was focused on obtaining the visual temperature distribution in the aluminium workpiece. The infrared radiation emitted from coated surface which characterizes the thermal energy distribution was detected by an IR camera. The IR images were recorded directly on the computer and converted with ThermaCAM Researcher computer

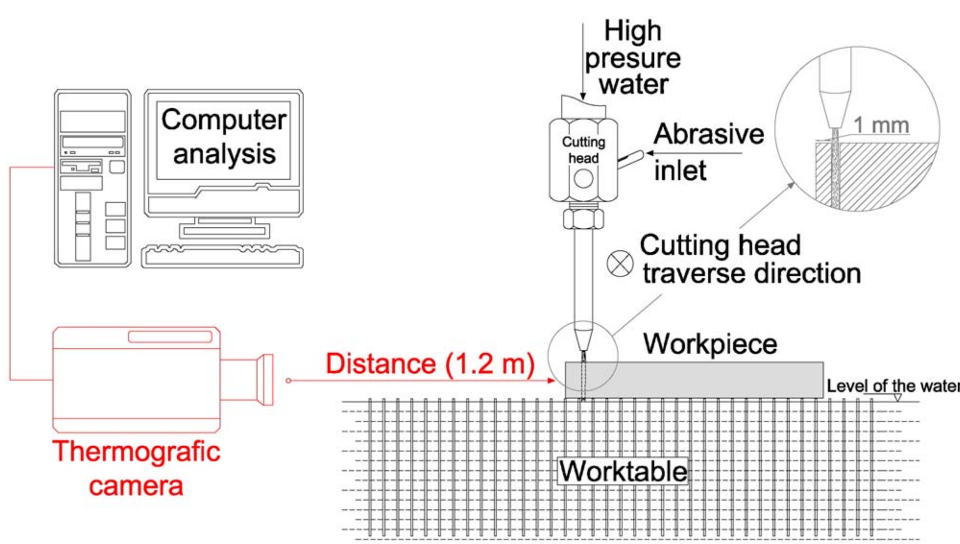

Fig. 1. Schematic of the experimental setup.

Table 1
Workpiece material properties.

Material	ISO: AlMg1SiCu, Aluminium 6061-T6
Material components properties	Al 98%, Cr 0.004–0.35%, Cu 0.15–0.4%, Fe max 0.7%, Mg 0.8–1.2%, Mn max 0.15%, Si 0.4–0.8%, Ti max 0.15%, Zn max 0.25%
Thermal properties	Thermal conductivity: 167 W m^{-1} K^{-1} Density: 2.7 kg m^{-3} CTE, linear 20 °C: 23.6 μm/m °C
Mechanical properties	Ultimate tensile strength: 310 MPa Fatigue strength: 96.5 MPa Tensile yield strength: 276 MPa Modulus of elasticity: 68.9 GPa Hardness, Brinell: 95.0

program (FLIR Systems, USA) into Matlab (The MathWorks, USA) data file for further analysis, which is explained in the next section.

3. Results and discussions

During cutting process IR camera recorded sequence of thermograms, which exhibit typical characteristics of AWJ processing, i.e. curved cutting front formation due to water jet energy dissipation during cutting. In order to show correspondence or even to confirm functional relationship between IR monitoring results and resultant workpiece surface quality, surface texture was evaluated by digital image processed macrophotography and compared to thermograms.

3.1. IR thermograms evaluation

Thermogram is an array of values with functional relation to temperature of the observed object. In contrast to visible imaging method which captures a two-dimensional function of the form $f(x, y) = i(x, y)r(x, y)$, where $i(x, y)$ is determined by the illumination source and $r(x, y)$ is determined by the reflection characteristics of the imaged objects [7], thermogram f_T generation can described by:

$$f(x,y) = \varepsilon(x,y) \cdot \tau \cdot T(x,y) + f_{re\,fl} + f_{atm} \quad (1)$$

where f_{refl} is a contribution of background IR radiation, reflected from the observed object, f_{atm} is a contribution of surrounding atmosphere, $T(x, y)$ is a temperature 2D scalar field, τ corresponds to transmittance of the atmosphere and $\varepsilon(x, y)$ is a local emissivity of the observed object. With proper calibration process and known emissivity of measured object, thermogram is a 2D array or matrix of temperature values on the measured object, which can be tackled by usual digital image processing methods.

The IR thermograms acquired during experiments described in this paper were collected to a sequence of images with framerate of 25 frames per second. Five selected frames out of complete sequence are shown in Fig. 3.

IR camera captured wider scene than just workpiece as can be seen in Figs. 2 and 3 therefore a location of AWJ cutting head was determined for each frame by discrete correlation of thermogram f_T and smaller thermogram of cutting head. The correlation matrix element with maximal value corresponds to location of the cutting head.

The area occupied by the workpiece in the thermogram was determined manually by computer pointing device (mouse) click on the two diagonal corners of the workpiece image in the figure on the computer screen. Coordinates of the clicks determined the image submatrix which belongs to the workpiece. Since the workpiece and the camera remained fixed during the experiment it was necessary to manually determine the workpiece position only on single frame. Example of the workpiece thermogram, extracted from wider scene can be observed in Fig. 4. Thermogram exhibits a

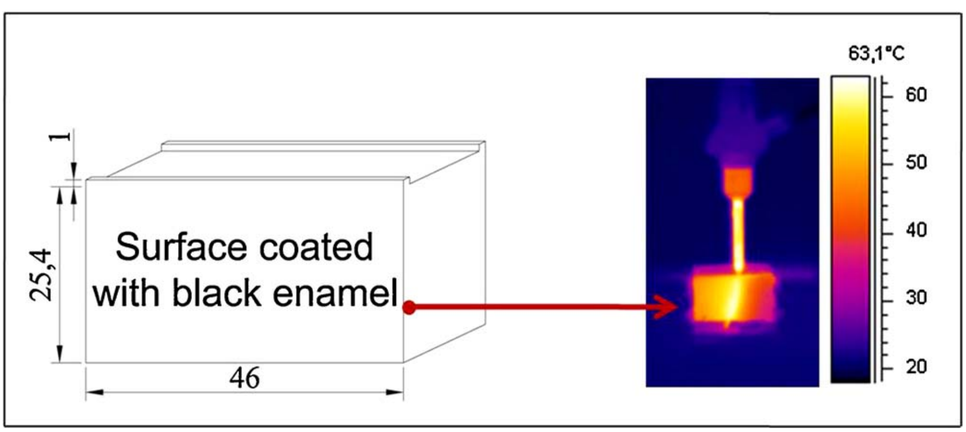

Fig. 2. Workpiece shown schematically with coated surface and thermogram with cutting head and workpiece.

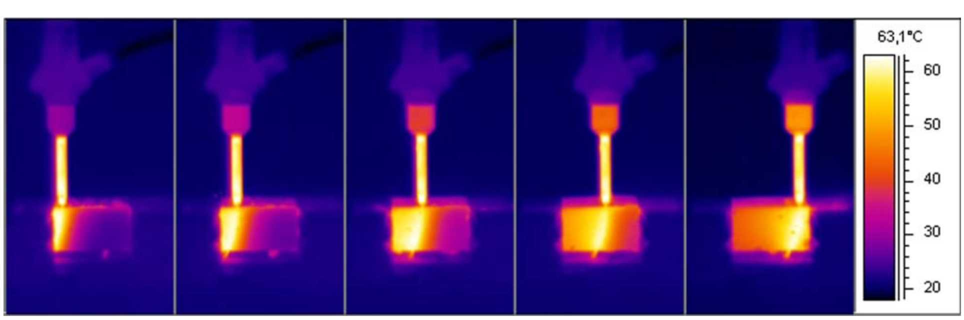

Fig. 3. Selected frames from the recorded sequence of IR thermograms.

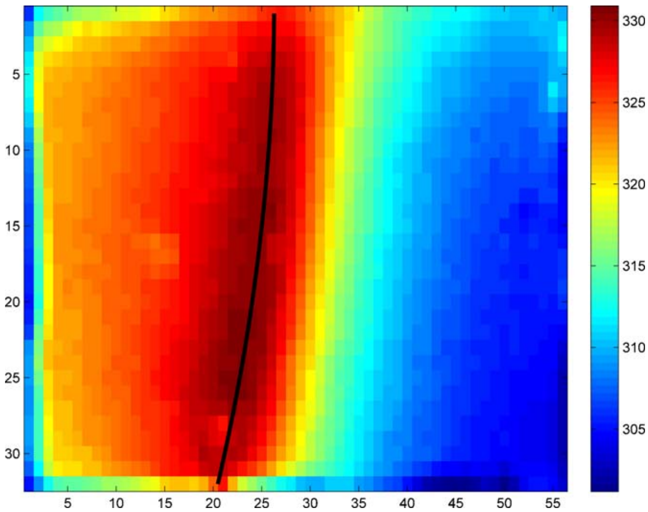

Fig. 4. ROI in the thermogram with fitted line corresponding to cutting front.

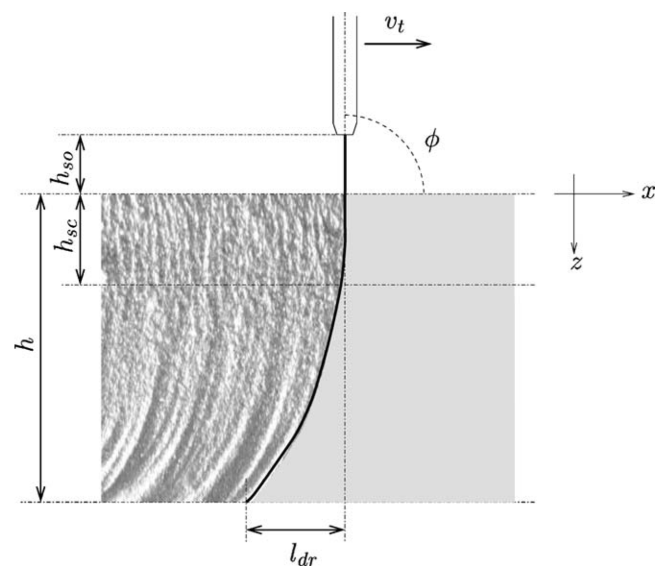

Fig. 5. Workpiece surface with characteristic texture, where v_t is the cutting head traverse velocity, ϕ is the impact angle of the jet, h_{so} is the cutting head stand-off distance, h is the thickness of the workpiece, h_{sc} is the depth of the smooth cutting zone and l_{dr} is the leg of AWJ at the bottom of the workpiece.

cutting front shape typical for water jet process. In order to numerically describe the cutting front shape a computer program searched through the lines of thermogram and identified the coordinate of hottest spot in the line. A polynomial of the second order was fitted with constraints to the set of hot spot coordinates, using Matlab function mmpolyfit [8]. The fitting was constraint with demand that slope of the cutting front is parallel to the water jet direction at the top surface of the workpiece, therefore the second coefficient of the polynomial is always zero, and the constant term equals to location of the abrasive water jet cutting head. In Fig. 4 region of interest (ROI) in the thermogram with fitted line corresponding to cutting front can be observed.

Procedure was repeated automatically on every frame in the series of thermograms, which were acquired with frequency 25 frames per second. Coefficients were stored for further correlation with surface texture characteristics.

3.2. Surface texture evaluation

Geometric situation during AWJ machining and related geometric parameters can be observed in Fig. 5. Surface texture shows two characteristic zones. With respect to the depth from the top of the cut, one can distinguish between upper 'smooth cutting zone' and 'rough cutting zone', where striations are much more pronounced. Based on visualization of the cutting front experiments and geometrical energy dissipation model, we can firmly state that striation geometry is strongly related to erosion mechanisms in the cutting kerf [9].

It was shown that second order polynomial can be found to describe a relation between the striation drag x and the depth of cut z:

$$z = f(x) = ax^2 + bx + c \qquad (2)$$

In this work surface texture characteristics were experimentally acquired by macrophotography and digital image processing with computer program SEMAC [9], written in Matlab. For image acquisition a camera CV-025 and corresponding machine vision system CV-2600 (KEYENCE, Japan) was used. To emphasize texture marks chosen suitable lightning conditions has been chosen, i.e. the light incident angle was set to 15°.

In order to obtain binary image, i.e. pure black and white, a threshold procedure was applied to acquire greyscale image. Every binary image was segmented to labelled objects. At this point it was rather trivial to determine the size of objects and to recognize larger objects as striation marks. Five objects were selected on each image and a constrained second order polynomial (Eq. (2)) was fitted on a set of image elements. Constraints used were identical

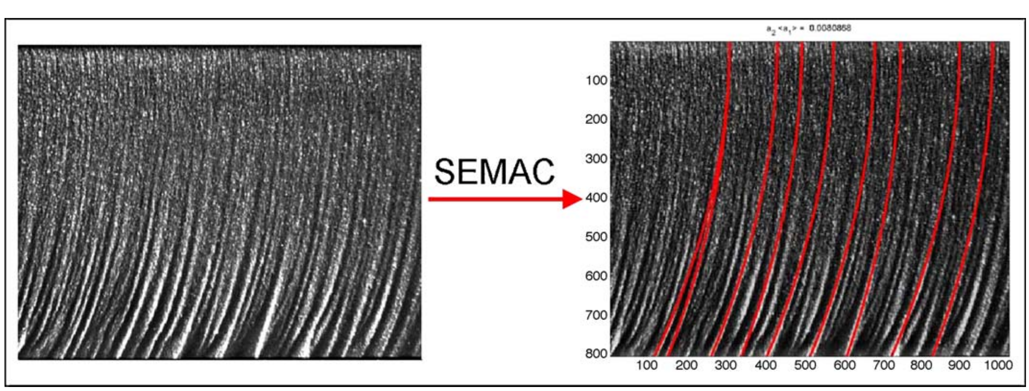

Fig. 6. Surface macro photography with several plots (in red color) of fitted polynomial after processing with SEMAC [9] software. (For interpretation of the references to color in this figure legend, the reader is referred to the web version of the article.)

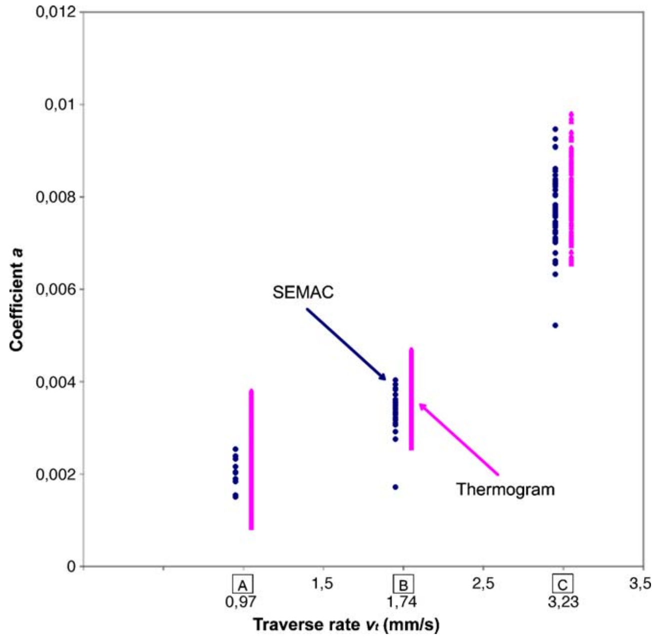

Fig. 7. Relation between AWJ cutting head traverse velocity and texture curvature leading coefficient a.

as in the case of evaluation of thermograms, i.e. the slope of the fitted second order polynomial should be zero at $z = 0$. The original greyscale image can be observed on the left side in Fig. 6, while on the right side several plots of fitted polynomials are superimposed on the original greyscale image. Leading coefficients of the fitted polynomials were stored for further correlation with characteristics of thermograms. Fitted lines resemble the shape of the cutting front well and therefore promise, that the leading coefficient in Eq. (2) could be used as a AWJ performance index.

Table 2
AWJ cutting process parameters.

Process parameter	Unit	Level	Value
Cutting head traverse rate v_t	mm/s	A	3.23
		B	1.74
		C	0.97
Water pressure, p	MPa		300
Orifice diameter, d_o	mm		0.25
Stand-off distance, h_{so}	mm		2.5
Abrasive GMA, mesh	#		80
Abrasive mass flow rate, Ma	g/s		5.3

Results obtained by experimental setup presented in Fig. 1 and texture evaluation as shown in Figs. 5 and 6 are summarised in Fig. 7. Experiments were performed at three different cutting head traverse velocities v_t, labelled in Table 2 and Fig. 7 with A, B and C.

In Fig. 7 results of microphotography texture evaluation and thermographic evaluation are plotted for A, B and C level of velocity versus leading coefficient of second order polynomial (coefficient a). At each level the left set of points (in blue color) correspond to texture evaluation and right set of points (in red color) to the thermographic online monitoring. It can be clearly observed, that

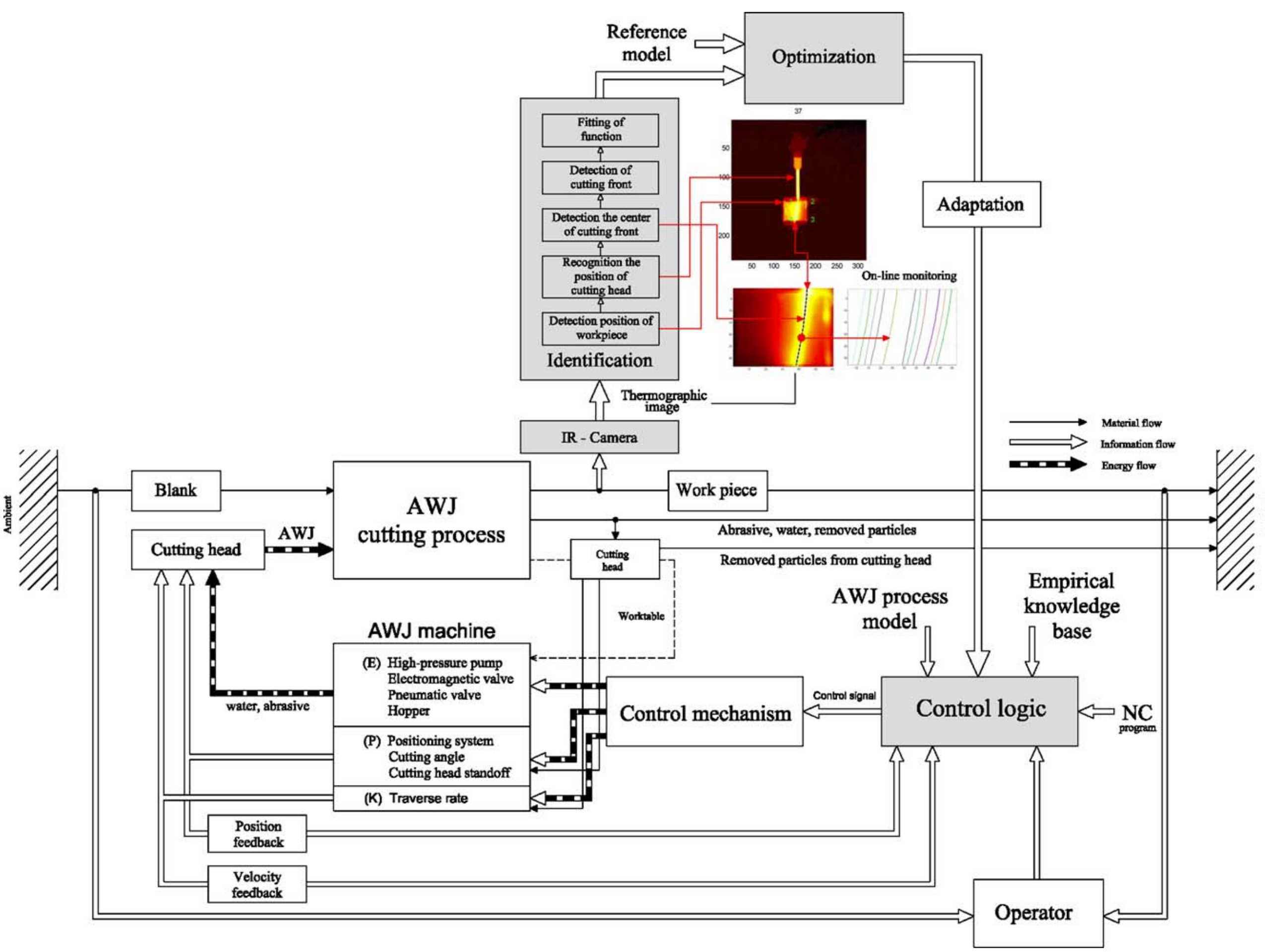

Fig. 8. Scheme of AWJ cutting system as a cybernetic structure.

by increasing the cutting head traverse rate v_t, leading coefficient of the quadratic function (Eq. (2)), fitted to the hottest points in the part of thermogram corresponding to workpiece, increases.

The increase is equal as in the case of observation with IR camera as in the case of surface texture evaluation. The dispersion of results is much higher in the case of online evaluation due to the stochastic nature of the AWJ machining process.

The purpose of the research was to prepare the monitoring methodology as a first step towards the control loop based on the process identification with IR thermography. The nature of AWJ machining process hinders to monitor the process by more direct methods, such as optodynamic [12]. AWJ cutting system cybernetic structure based on work of Peklenik [10] and Zaletelj et al. [11], supplemented with process performance monitoring based on IR thermography is presented in Fig. 8. The concept of monitoring part is modular so as to enable flexibility of various sensing methods in the future.

4. Conclusion

Experiments of AWJ cutting process monitoring by IR thermography has been performed and results reported in this paper. It has been shown, that process performance index can be online extracted from the thermographic images. Credibility of process performance index has been validated by texture evaluation on machined surfaces by macrophotography and digital image processing. It can be anticipated that applicability of the proposed system is mainly in laboratories where technological databases are being researched. Described monitoring system can shorten tedious experimentation procedures. Based on these results a cybernetic structure for AWJ machining control system has been proposed which will enable AWJ machines to work more autonomous.

Acknowledgments

This work is supported by the mainframe of the project ‘‘Innovative production systems’’, contact number P2-0248 (C) financed by MVZT of RSLO and by the ‘‘Multi-Material Micro Manufacture: technology and Applications (4M)’’ Network of Excellence, Contact Number NMP2-CT-2004-500274.

References

[1] Hashish, M., 1988, Visualization of the Abrasive Waterjet Cutting Process, Experimental Mechanics, 28/2: 159–169.
[2] Ramulu, M., 1993, Dynamic Photoelastic Investigation on the Mechanics of Waterjet and Abrasive Waterjet Machining, Optics and Lasers in Engineering, 19/1–3: 43–65.
[3] Ohadi, M., Ansariand, A.I., Hashish, M., 1992, Thermal Energy Distributions in the Workpiece During Cutting with an Abrasive Waterjet, Journal of Engineering for Industry, 114/1: 67–73.
[4] Kovacevic, R., Mohan, R., Beardsley, H.E., 1996, Monitoring of Thermal Energy Distribution in Abrasive Waterjet Cutting Using Infrared Thermography, ASME Journal of Manufacturing Science and Engineering, 118/4: 555–563.
[5] Zeng, J., Olsenand, J., Olsen, C., 1999, The Abrasive Water Jet as a Precision Metal Cutting Tool, 10th American Water jet Conference, vol. 10, pp.14–17.
[6] FLIR Systems. 2006, User's Manual ThermaCam S65, FLIR Systems.
[7] Gonzales, R.C., Woods, R.E., 2002, Digital Image Processing, Prentice-Hall, New Jersey.
[8] Hanselman, D., Littlefield, B., 2005, Mastering MATLAB 7, Prentice-Hall, Pearson.
[9] Lebar, A., Junkar, M., 2001, Surface Evaluation Methods for Advanced AWJ Cutting Techniques, Manufacturing Systems, 31:101–103.
[10] Peklenik, J., 1988, Fertigungskybernetik – eine neue wissenschaftliche Disziplin fur die produktionstechnik, Sonderdruck der TU Berlin, 1–25.
[11] Zaletelj, A., Sluga, A., Butala, P.A., 2008, Conceptual Framework for the Collaborative Modeling of Networked Manufacturing Systems. Concurrent Engineering, Research and Applications, 16/1: 103–114.
[12] Bračun, D., Diaci, J., Možina, J., 2001, Optodynamic Measurement of a Nonstationary Temperature Field in Air by Multiple Laser-beam Deflection, Measurement Science & Technology, 12/11: 2009–2014.